Doi:

The role of pulmonary mast cells activation and degranulation in the process of increased pulmonary artery pressure

Jie Liu[1,2], Shuang Ma[1], Qiaorong Ji[1], Chengzhu Cao[1], Ying Han[1,2], Xiaozhou Wang[1,3] and Wei Zhang[1]

[1] *Research Center for High Altitude Medicine, Key Laboratory for High Altitude Medicine, Ministry of Education, Qinghai University, Xining 810001, China*
[2] *Department of pathophysiology, Medical College, Qinghai University, Xining 810001, China*
[3] *Qinghai Cardio-Cerebrovascular Hospital, Xining, 810001, China*

Short title: Pulmonary mast cells activation with increased PAP
Liu et al.

Correspondence to: Wei Zhang, Research Center for High Altitude Medicine, Key Laboratory for High Altitude Medicine, Ministry of Education, Qinghai University, Xining, Qinghai, China
E-mail: zw0228@qhu.edu.cn

Abstract. Hypoxia exposure often cause the increases of pulmonary arterial pressure (PAP). Studies reported that mast cells (MCs) participate in pulmonary vascular remodeling and promote the formation of chronic pulmonary hypertension. Current studies mainly focus on the change of MCs under chronic hypoxia, but few studies on the regulatory role and mechanism of MCs under acute hypoxia. Therefore, present study investigated the dynamic change of MCs in lung tissues under acute hypoxia and the role of MCs activation in the increasement of PAP. In our study, we established an experimental rat model of acute hypobaric hypoxia using a hypobaric chamber (simulated altitude of 7,000m) and pretreated with MCs degranulation inhibitor Sodium cromoglycate (SCG) to study the MCs changes under acute hypoxic exposure. We found that acute hypobaric hypoxia contributed to the increased quantity, activity, and degranulation of MCs and SCG pretreatment showed attenuated PAP elevation under acute hypoxia. Our findings implied that there is a possible mechanism of acute hypoxia cause rapid recruitment of MCs, activation, and explosive degranulation to release Tryptase, Chymase, IL-6, His, 5-HT, and Ang II, which further contributed to pulmonary microvascular contraction and increase in PAP. This work extends the knowledge about MCs, providing a potential profile of MCs as an alternative treatment for high altitude pulmonary edema (HAPE) related increased pulmonary artery pressure.
217 slov

Key words: Acute hypoxia — Pulmonary arterial pressure — MCs — Sodium cromoglycate

Abbreviations: Ang II, ngiotensin II; HAPE, high altitude pulmonary edema; His, histamine; HPV, hypoxie pulmonary vasoconstrietion; 5-HT, 5-hydroxytryptamine; IL-6, interleukin-6; MCs, mast

cells; SCG, sodium cromoglycate/sodium cromolyn; SD rats, Sprague-Dawley rats; PAP, pulmonary artery pressure

The list of abbreviations in experiments

Method	Group name	Group name explanation
TB (Toluidine Blue) stain	NC -3,6,12,24 h group	2,26 0m,3, 6, 12, 24h (Xining, 2,260m, for 3, 6, 12, 24h)
	HC -3,6,12,24 h group	7,000 m,3, 6, 12, 24h (hypobaric chamber, simulated 7,000m, for 3, 6, 12, 24h)
TEM (Transmission electron microscopy)	NC-12h	2,260 m, 12 h
	HC-12h	7,000 m, 12 h
WB（Western blot）assay	N12C	2,260 m + NS , 12 h
	H3,6,12C	7,000 m + NS, 3, 6, 12h
	N12S	2,260 m + SCG ,12 h
	H3,6,12S	7,000 m + SCG, 3, 6, 12h
IF and Elisa assay	NC	2,260 m+NS, 12h
	NSCG	2,260 m+SCG, 12h
	HC	7,000 m+NS, 12h
	HSCG	7,000 m+SCG, 12h
Monitoring of PAP	20.9%O_2+NS	2,260 m, 20.9 % O_2+ NS
	15% O_2+NS	2,260 m, 15%O_2 + NS
	20.9% O_2+SCG	2,260 m, 20.9 % O_2+ SCG
	15% O_2+SCG	2,260 m, 15%O_2 + SCG

Introduction

Generally, environment hypoxia plays vital role in the occurrence of various acute and chronic altitude illnesses (Burtscher et al. 2014, Luo et al. 2014). Acute hypoxia can cause pulmonary arterial pressure (PAP) increases, and even cause high-altitude pulmonary edema (HAPE) in severe cases further threaten the life of the patient (Li et al. 2018, Luks et al. 2019). The increase of PAP under acute hypoxic is caused by pulmonary vasoconstriction and pulmonary circulation resistance, the complex mechanism involves vascular response, neuromodulation, immune response, biochemical metabolism, genetic expression, molecular signal transduction and other abnormalities (Mandegar et al. 2004).

In recent years, there are increasing interests on the pathophysiology of immune injury , as well as the prevention and treatment targeting the immuno-injury in various type of hypoxia related altitude diseases. Mast cells (MCs) monitor the innate immunity and regulate acquired immunity, further act as an important immune cell compartment during type I allergic response. MCs are involved in various biological functions (Puxeddu et al. 2005). Currently, there is increasing amount

of evidences verify the core role MCs in acute inflammation (Puxeddu et al. 2005), T cells reaction (Lotfi-Emran et al. 2018), fibrosis (Levick & Widiapradja 2018), nervous system injury (Hendriksen et al. 2017), angiogenesis (Ribatti et al. 2019) etc. In the lung tissue, MCs are distributed in the pulmonary microvessels, submucosal mesenchyme of the trachea, smooth muscles and mucous glands. This special distribution conveys the possibility that MCs play an important "sentinel" role in supervision of lung immune microenvironment (MacLean & Dempsie 2009). MCs contain with various mediators, such as granule-associated mediators, lipid-derived mediators, cytokines and chemokines etc., they all together help to prevent the local microenvironment from invading pathogen and injury from the immune response (Chumanevich et al. 2016). Typically, hypoxia has been largely reported to modulate MCs, study showed that MCs response to Staphylococcus aureus infection is modulated by hypoxia (Möllerherm et al. 2017).

Over the past decades, increasing evidences confirmed that the role of MCs in the development of pulmonary arterial hypertension (PAH). MCs are well known as the "catalysts" of pulmonary vascular remodeling in chronic PAH (Rhind et al. 1986, Vajner et al. 2006, Novotný et al. 2015, Aiello et al. 2017,). An example of this is the study carried out by Kosanovic D in which abundant perivascular MCs were present in the lungs of patients with PAH and experimental models of pulmonary hypertension (Kosanovic et al. 2014). In a similar case, a study conducted by Jian Xu implied a crucial role of MCs in the remodeling of pulmonary vessels through dynamic viewing of MCs in PAH (Xu et al. 2018). These studies mainly focused on the role of MCs under chronic hypoxic conditions. So far, there has been little discussion about the modulation of MCs and their mechanism exposed to acute hypoxia.

MCs degranulation inhibitor Sodium cromoglycate / Sodium cromolyn (SCG) is a MCs membrane stabilizer, which prevent MCs to release intracellular compartments. The effect of SCG on MCs degranulation is tissue-specific, and it can inhibit MCs to release mediators in lung tissues. Therefore, it was selected as a tool drug in our experiment. We pretreated the Sprague-Dawley (SD) rats with SCG and investigated the change of pulmonary MCs under acute hypoxia and the role of MCs activation and degranulation in the process of increased PAP.

Materials and Methods

Animals and ethics statement

A total of 184 healthy male SD rats (271.55±22.43 g) with SPF grade were provided by Nanjing Qing long-shan Animal Breeding Farm (Jiangsu, China). Its license number was SCXK (Su) 2017-0001. Its qualified certificate number (201803296) was also obtained after detection by Suzhou University. All procedures throughout this study were done in accordance with the People's Republic of China (PRC) National Standard-Laboratory animal Requirement for quality control (GB/T 3491-2017) and were approved by the Ethics Committee of Medical College of Qinghai University. Rats were maintained in the animal house of Medical College of Qinghai University under the following laboratory conditions: altitude of 2,260m (P 77.43KPa, PO_2 15.75 KPa), clean and ventilated feeding hood, temperature of 24±2°C, and 12:12 h light/dark cycle. These rats had free access to standard maintenance pelleted food purchased from Beijing Ke’ao Xieli Feed CO.,

LTD. (Beijing, China) and water ad libitum. Animals were transported to the testing laboratory and retained there for 1 h for adaptation and acclimatization before the experimental time settings.

Instruments and reagents

The main instruments and reagents used in this work were as listed below: HCP-Ⅲ D800 low-pressure simulation cabin for experimental animals (Φ140cm*80cm, Xi'an Fukang Air Purification Equipment Engineering Co., Ltd., China); automatic dehydration instrument for paraffin specimen (Shadon Pathcentre Company, UK); paraffin embedding machine (Leica EG1150H,Germany); paraffin microtome (Leica RM2265,Germany); Fluorescence Microscope (Nikon Eclipse C1, Japan / Leica DM4B,Germany,); sodium pentobarbital (Catalog: 071025; Shanghai Tyrrell Company, China; SCG (Catalog: C0399-1G; Sigma Company, USA); Toluidine blue (TB) staining kit (Catalog: D034; Nanjing Jian cheng Company, China); Tryptase , Chymase , β-actin antibody,Goat Anti-Mouse and Goat Anti-Rabbit IgG (HRP), goat F(ab) 2 anti-mouse IgG-Fc (PE) and goat anti-rabbit H&L (FITC) were purchased from Abcam company, UK. ELISA Kit (IL-6, His, Ang II, 5-HT) were purchased from Elsbscience Company, China.; microplate reader (Thermo Fisher Scientific, USA); ML818 PowerLab biological signal data acquisition and analysis system (AD Instruments, Australia); MLT0380/A pressure sensor (AD Instruments, Australia); small animal ventilator (Columbu Instrument, USA); NJ 07013 automatic constant temperature heating plate (Physitemp Instruments, Inc., USA).

Animal grouping

Model construction induced by acute hypobaric hypoxia

According to the preliminary experiment, we established a rat model of acute hypobaric hypoxia using a hypobaric chamber (simulated altitude of 7,000m, P 39.84KPa, PO_2 7.57 KPa) to study the activation and degranulation of pulmonary MCs under acute hypoxic stimulation.

Conditions optimized for SD rats model induced by hypobaric hypoxia by Toluidine blue (TB)staining and Transmission electron microscopy(TEM).

To explore the changing trend of pulmonary MCs under acute hypobaric hypoxia exposure and the conditions of hypoxia exposure time. Forty-eight SD rats were randomly divided into two groups (n=24): NC group (Xining, 2,260m, P 77.43KPa, PO_2 15.75 KPa) and HC group (hypobaric chamber, 7,000m, P 39.84KPa, PO_2 7.57 KPa), which divided into four groups depending on the exposure time separately (3, 6, 12, 24h). Concretely, after being labeled with picric acid, animals in NC group were placed in the animal breeding room at an altitude of 2,260 m, while those in HC group were placed in hypobaric chamber at a simulated altitude of 7,000 m for 3, 6, 12, and 24 h. The lung tissues of rats were sectioned in paraffin. TB staining was used to observe the trend of changes in the number lung MCs and explore the relatively high activation time of pulmonary MCs which further perform TEM experiments to observe the ultrastructure of lung tissues (especially MCs).

Conditions optimized for SCG pretreatment SD rats model induced by hypobaric hypoxia by WB (Western blot) assaying

To evaluate the tendency of SD rat lung MCs activation and degranulation under different acute hypoxia exposure times after SCG pretreatment. Forty-eight SD rats were randomly divided into four groups (n=24): N12C group (n=6, Xining, 2,260 m + NS ,12 h); N12S group (n=6, Xining, 2,260 m + SCG ,12 h); H3,6,12C group (n=18, hypobaric chamber, 7,000 m+ NS, 3,6,12h); H3,6,12S group (n=18, hypobaric chamber, 7,000 m + SCG,3,6,12h), HC group and HS group, which divided into three groups (n=6) depending on the exposure time separately (3, 6,12h) and two normoxic 12h groups which with (N12S) or without SCG (N12C). Animals in each group were treated with NS or SCG 100 mg kg^{-1}. ip. Fresh lung tissues from each group were sampled for WB assays. WB was used to determine the expression of MCs-specific proteases Tryptase and Chymase.

To clarify the changes in pulmonary MCs activation and degranulation under acute hypobaric hypoxia exposure by immunofluorescence(IF) and enzyme-linked immunosorbent assay (*ELISA) assaying*

Forty-eight SD rats were randomly divided into four groups (n = 12): NC group (2,260 m+NS), NSCG group (2,260 m+SCG), HC group (7,000m+NS), HSCG group (7,000m+SCG). Animals in each group were treated with NS or SCG 100 mg kg^{-1}. ip. as designed. Afterwards, animals in NC and NSCG groups were placed in animal breeding room at an altitude of 2,260 m for 12 h, while those in HC and HSCG groups were placed in hypobaric chamber at a simulated altitude of 7,000 m for 12 h. Half of the animals in each group were fixed by perfusion and the rest were used for fresh tissue extraction. IF was used to observe the distribution and percentage of Tryptase (red) and Chymase (green) positive cells in lung tissues of each group and ELISA was used to detect the expression of Interleukin-6 (IL-6),5- hydroxytryptamine (5-HT), Histamine (His) and Angiotensin II (Ang II) for identify the activation, degranulation, release of inflammatory factors and vasoconstrictors under acute hypoxia stimulation.

Animal grouping and model construction induced by acute normobaric hypoxia by PAP monitoring

To determine the role of MCs activation and degranulation in the process of increasing PAP under acute normobaric hypoxic stimulation. A ventilation experiment 15% O_2 (Xining, 2,260 m, P 77.43KPa, $PO_2$11.64KPa) versus 20.9% O_2 (Xining, 2,260m, P 77.43KPa, PO_2 15.75 KPa). Forty SD rats were randomly divided into four groups (n = 10): 20.9%O_2+NS group, 15% O_2+NS group, 20.9% O_2+SCG group, 15% O_2+SCG group. SD rats in SCG and NS groups were pretreated 30min before being put into the hypobaric chamber with SCG (100 mg kg^{-1}.ip) , respectively. The PAP was dynamically monitored when the right external jugular vein was cannulated to the pulmonary artery.

Methods

Lung tissues sampling by perfusion fixation

Animals were anesthetized with sodium pentobarbital (60 mg kg^{-1} ip) after completing remodeling, the trachea was intubated, and the lungs were inflated with 10 cm H_2O pressure of positive pressure before being deflated to 5 cmH_2O for perfusion with saline solution after cannulation of the pulmonary artery and cut the left atrium open. Perfusion was carried out for removal of blood from the pulmonary circulation, followed by the TEM fixative /4% PFA for 10 min. The lower half of the left lung tissue were collected for TEM, TB staining or IF assays

Fresh lung tissues sampling

Animals were anesthetized with sodium pentobarbital (60 mg,kg^{-1}). ip. and the lung tissue were then immediately collected and frozen in liquid nitrogen and stored in -80℃ freezer awaiting WB and ELISA assays.

TB staining

TB staining was employed to evaluate the density and degranulation of MCs. The paraffin sections were stained with 0.1% TB for 10 seconds. The morphology and distribution of TB-positive cells (fuchsia, MCs indicators) were observed under a light microscope. A total of 5 high-powered fields with pulmonary microvessels were randomly selected in each slide, and the total number of TB-positive cells (MCs) in these five fields were counted, and the final quantity of each group was the average of the total number of MCs in 6 slices.

TEM experiment

After fixation, the lungs were excised and stored in glutaraldehyde at 4°C. Lung tissues were cut into small cubes (1-1.5mm^3), which were embedded in Araldite. A 1 μm thick semi-thin section was made and stained with TB to locate MCs. Ultrathin sections (50–70 nm) were cut , contrasted with uranyl acetate and bismuth subnitrate. The ultrastructure of lung tissue (especially MCs) was performed observed by TEM.

WB assaying

Total protein was extracted and quantified. The sample and protein marker were separately loaded. SDS-PAGE was electrophoresed at a constant voltage of 80 V and 120 V. Thereafter, the gel was carried out to load on PVDF membrane soaked in methanol. The transfer clip was placed into the transfer tank and membrane was transferred for 2 h at 350 mA. Incubated blocking solution for 1 h , the primary antibody diluent (1:1000) was added in. The sample stayed overnight at 4℃. After that, the secondary antibody diluent (1: 5000) was added and incubated for 1 h. Finally, ECL luminescent liquid was added on membrane, which was subsequently transferred into the luminescence imager. Three exposures were taken and the β-actin was blotted as the loading control.

IF assaying

After being deparaffinized and hydrated, paraffin sections received antigen retrieval under high pressure, and were blocked with 10% goat serum. Thereafter, they were incubated overnight at 4°C

in the addition of Chymase/ Tryptase antibody (1:100). After being washed with water, goat F (ab) 2 anti-mouse IgG-Fc (PE) fluorescent secondary antibody (red) and goat anti-rabbit H&L (FITC) fluorescent secondary antibody (green) were added in. Soon after, the slide was sealed after dropping the DPAI. The section was finally scanned and the percentage of red and green light-positive cells (%) was separately calculated by HALO analysis software.

ELISA assaying

IL-6, 5-HT, His and Ang II ELISAs assay were performed in accordance with the manufacturer's guidelines. After the reaction, the optical absorbance (OD) was recorded at 450 nm on the microplate reader.

Real-time and dynamic monitoring of PAP

Our research group has verified that 15% O_2 ventilation has successfully replicated the model of acute normal pressure hypoxia in SD rats (Zhang et al. 2009; Ji et al. 2020). Animals in each group were anesthetized with 2.5% sodium pentobarbital (50 mg kg^{-1}, ip), then fixed supinely on the constant heating plate. The trachea was intubated to connect to a ventilator (respiratory rate of 70 breaths min^{-1}, tidal volume of 7 ml kg^{-1} and a positive end-expiratory pressure (PEEP) of 2.5 cmH_2O. The right external jugular vein was cannulated (A polyethylene catheter: OD. 0.96 mm, ID. 0.8 mm) and connected to the PowerLab biosignal acquisition system. With the help of tracing chart, cannula was delivered into pulmonary artery orifice in the right ventricular for dynamic monitoring PAP. The left femoral vein was cannulated (OD. 0.96mm, ID. 0.58 mm) for delivery of SCG or NS (100 mg kg^{-1}). After 10 minutes of injection, *20.9% O_2 group* was ventilated with air (20.9% O_2, P 77.43KPa, PO_2 15.75 KPa; Xining, China) and 15% O_2 group was ventilated with gas containing 15% O_2 (85% N_2, 15% O_2) (2,260, P 77.43KPa, PO_2 11.64KP; Xining, China, configured with nitrogen (N_2) diluted air, checked and calibrated by PowerLab system). At the same time, PAP changes received continuous, real-time and dynamic monitoring by PowerLab biological information acquisition system at 200 Hz sampling frequency. The PAP values of each animal at baseline, 0, 0.5, 1.0, 1.5, 2.0, 3.0, 4.0 and 5.0 minutes ± 5 seconds were recorded. Data took the average value of maximum PAP wave.

Statistical analysis

All analyses were carried out using SPSS 18.0 software. Data were shown as mean ± standard deviation. Student's t test was applied to analyze the significance differences between two independent groups. One-way ANOVA was used for multi-group comparisons, and SNK-q (Student-Newman-Keul) test was used for the pairwise comparison of the any two groups mean, $P<0.05$ was considered statistically significant.

Results

At the beginning of this work, animal remodeling induced by acute hypobaric hypoxia or acute normobaric hypoxia was separately established for testing. As for acute hypobaric hypoxia, animal

hypobaric chamber was established by simulated altitude of 7,000 m. Lung tissues were immediately collected after animal leaving this chamber so as to obtain ideal experimental samples for hypoxic stimulation. This model was not employed to monitor PAP for the possibility that animals were exposed to normoxia after leaving the chamber, making PAP deviated from the hypoxic stimulus. In terms of acute normobaric hypoxia, SD rats were fully anesthetized and their tracheal intubation was connected to a ventilator with hypoxic air mixture containing 15% O_2. This model was only used for monitoring PAP in real-time, but not for lung tissue extraction to avoid the effects of anesthesia, surgical operations, and intubation on them. Both models are designed for the purpose of this study, and the using of SCG drugs achieved the ultimate goal of the study.

TB staining results of lung tissue

TB staining is a MCs specific staining method (Ribatti , 2018). The color differs in the number of MC granulescells present elliptical or round in large size with deep staining represent the greater number of granules. In contrast, light stained cell with irregular shape and decreased size represents MCs degranulation. As shown in Figure 1A, only trace amounts of MCs in small size were occasionally observed in lung tissues from NC groups at varied hypoxia exposure times (3, 6, 12, and 24 h). Diametrically, close inspection of Figure 1A showed more and larger MCs in lung tissues from HC groups compared to N groups. They were mostly single-, multiple- or clusters-like distribution near the pulmonary microvessels, the submucosal mesenchyme of the trachea, the lung capsule, and the alveoli. Moreover, they were in different shapes and sizes as well as some degranulation. Through statistical analysis, TB positive cells were correspondingly counted and analyzed. From Figure 1B, TB staining showed that at the same time, the number of TB-positive cells in each group of HC was more than that of group NC (P >0.05). The HC groups had significantly different number of TB positive cells with all the different time point of hypoxia treatment. More specifically, the TB-positive cells among HC groups showed a trend of HC-12h >24h >6h >3h group (P <0.05). The MCs in HC groups at 12 h achieved the most abundant numbers. Nonetheless, no significant differences were observed among the NC groups at different time periods. Overall, these results indicated that acute hypobaric hypoxia promoted the MCs accumulation and the exposure time to hypoxia also had an effect on the accumulation. Our result demonstrated that exposure to acute hypoxia can facilitate the accumulation of MCs in lung tissue.

TEM results of lung tissue

According to TB staining results, NC-12h group (2,260 m, 12 h) and HC-12h group (7,000m,12 h) lung tissue was examined by TEM to observe the ultrastructure of lung tissues (especially MCs). Figure 2A presents the morphological characteristics of lung tissues harvested from the rats in the NC-12h group. In detail, they had thin alveolar wall, whose cyst wall was lined with two types of alveolar epithelial cells (type I and II). Alveolar type II epithelial cells were cubic with microvilli-like protrusions on the free surface of the cell. Moreover, their nucleus was in irregular shape, cytoplasm inside had abundant organelles and a large number of clear lamellar bodies, and rough endoplasmic reticulum was in short and rod shape. Blue arrows indicate normal lamellar

bodies in Figure 2A. However, MCs were not found in lung tissues from NC-12h group. Turning to the morphological characteristics of lung tissues derived from rats in HC-12h group compared with NC-12h (Figure 2 B-H), it was observed that the thickened alveolar sacs wall and the swolle alveolar epithelial cells. Alveolar type II epithelial cells had loose and broken lamellar corpuscles in the cytoplasm, with low electron density and changed vacuole emptying (Yellow arrows indicate damage and evacuation of lamellar bodies, Figure 2B, 2C). The mitochondria were swollen in oval or round shape and rough endoplasmic reticulum was in short and rod shape (Green arrows indicate the mitochondria swollen in oval or round shape， Figure 2C). In addition, the capillary endothelial cells were swollen, and a large number of macrophages, neutrophils, eosinophils and other inflammatory cells were observed in the capillary cavity and alveolar cavity (Pink arrow indicates erythrocyte, neutrophils, eosinophils et al. aggregated in capillaries, Figure 2D). The MCs appeared to be near the capillary cavity and the inner part of the alveolar had relatively large size and irregular shape of nucleus, in which the heterochromatin was distributed along the nuclear membrane. Furthermore, the cytoplasm of MCs was filled with enormous special granules, which were featured in uneven size and covered with envelopes from outside. The granules observed in MCs were mainly two kinds. One had uniform and fine characteristics, while the other had more fine and dense characteristics. Significantly, the outer membrane structure of some granules disappeared, as shown in Figure 2 E-H. TEM results showed obvious damage to lung tissues, especially alveolar type II epithelial cells, MCs filled with enormous special granules, acute hypobaric hypoxia exposure for 12 hours. Therefore, simulated altitude of 7,000 m and 12 h exposure to hypobaric hypoxia were selected as the optimized conditions of rat modeling.

WB assay results of lung tissue

To clarify the change trend of lung MCs activation after SCG pretreatment under acute hypobaric hypoxia exposure. Tryptase and Chymase have generally been considered vital granule-associated mediators for MCs (Atiakshin et al. 2019). Tryptase is a most abundant protein in MCs, and used as a specific activation marker for MCs activation and degranulation, which can directly reflect the change in the amount and activity of MCs. Chymase is also an important activation marker for MCs. The SD rats were pretreated using SCG, and then attention was paid to the Tryptase and Chymase results of WB assay (Figure 3A). The expression of Tryptase generally decreased ($P<0.05$), but Chymase had no significantly different in N12S group than N12C group. Expression of Tryptase (Figure 3B) and Chymase (Figure 3C) in H3C, H6C and H12C groups were increased when compared to N12C group ($P<0.05$). The expressions of Tryptase and Chymase in the HC group showed a trend of, H6C, H12C >H3C groups. This also suggested that acute hypobaric hypoxia contributed to the increased expression of Tryptase and Chymase as a result of enhanced MCs activation. After SCG pretreatment, expression of Tryptase and Chymase in H3S, H6S and H12S groups all showed decreasing trends compared with corresponding non-SCG treated H3C, H6C, and H12C group ($P<0.05$). There was no significant difference in the HS groups. According to these results, we used SCG pretreatment of 12h exposure in a hypobaric chamber as optimal experimental conditions of subsequent experiment in our study. Tryptase (Figure 3D) showed a trend of H12C >N12C > N12S , H12S groups ($P<0.05$). Chymase (Figure 3E) showed a trend of

H12C >H12S > N12C >N12S groups (P<0.05). From WB assay results suggested that Tryptase and Chymase were stably expressed from 6h to 12h under acute hypobaric hypoxia stimulation. Combined with the results of TB, TEM and WB assay of lung tissue, 12h exposure in animal hypobaric chamber (7,000m) after SCG pretreatment was selected for the optimal experimental conditions for subsequent hypoxic exposure in our research.

IF assay results

IF assay could provide a relatively visual presentation of the number, morphology, and distribution of MCs as well as the typing of MCs after acute hypoxic stress. In lung tissues, Tryptase and Chymase were represented in red and green respectively. Figure 4A revealed that Tryptase (red) and Chymase (green) positive cells in HC groups were predominately distributed compared with NC group, Tryptase and Chymase positive cells numbers and volume were increased in the HC groups. They were mainly distributed in single, multiple, or clusters near the pulmonary microvessels, the submucosal stroma of the trachea and the lung capsule with different shape and size, and Tryptase and Chymase were mostly present in the same cell. Moreover, the Tryptase and Chymase positive cells besides the microvessels in HSCG group were in relatively small size and low density compared to HC group. Tryptase (Figure 4B) and Chymase (Figure 4C) positive cells in the HSCG group were significantly lower than those in the HC group (P<0.05), and the percentage of positive staining of Tryptase and Chymase showed a trend of HC >HSCG >NC, NSCG group (P<0.05). These changes were clearly suggest that hypoxic stimulation significantly activates MCs (MC_T and MC_{TC} type, mostly MC_{TC} type) near pulmonary microvessels, and these MCs quickly play a "sentinel" protective role. WB and IF results implied that SCG could slow down the MCs activation as a result of acute hypobaric hypoxia through inhibiting MCs degranulation.

ELISA assay results of lung tissue

To better understand the function of MCs in lung tissues when exposed to acute hypobaric hypoxia, ELISA assays was performed to detect the common vasoactive modulators (IL-6, 5-HT, His and Ang II) in lung tissues from SD rats. Figure 5. Showed that the expression of IL-6, His and 5-HT in lung tissue of HC group was the highest, the NC group and NSCG group were the lowest, and the HSCG group was in the middle, showing a trend of HC group >HSCG group >NC, NSCG group (P <0.05) (Figure 5A, B, C) , and the content of Ang II was not significantly different between the HC group and the HSCG group (P >0.05), however, it was higher than that of the NC group and the NSCG group, showing a trend of HC group, HSCG group > NC, NSCG group trend (P <0.05) (Figure 5D). ELISA results implied that the pulmonary activated MCs released inflammatory mediator IL-6, and vasoconstrictors His, 5-HT and Ang II through degranulation.

PAP monitoring results

In order to evaluate the role of lung MCs activation and degranulation in the process of increased PAP, acute normobaric hypoxia treated rat model was established and their PAP data were continuously real time monitored. As it shows in Figure 6A. It was found that, compared with 0min,

the PAP increased after 1min in the 15% O_2+NS group , and the increase of PAP after 1 min was statistically significant ($P < 0.05$); Compared to 20.9% O_2+NS group， PAP increased at all time points in the 15% O_2+SCG group; PAP in the 15% O_2+SCG group was lower than 15% O_2+NS group at each time point, the PAP difference at 1.0, 1.5, 3.0, 4.0 and 5.0 min were statistically significant ($P < 0.05$) (Figure 6B). Therefore, it is was demonstrated that the pretreatment with SCG have the ability to decrease PAP in rats under acute hypoxia stimulation. Our findings implied that there is a possible mechanism of pulmonary MCs activation and degranulation under acute hypoxic stimulation further participate in the process and even promote the occurrence of increased PAP.

Discussion

Hypobaric hypoxia environment of plateau often contributes to HAPE, PAP increases becomes the hallmark of HAPE (Maggiorini 2010). The previous researches on HAPE suggests that it is highly associated to acute PAP increases (Li et al. 2018, Luks et al. 2019). Numerous studies demonstrate that MCs play a role in development of chronic PAH. However, the role of of MCs in acute PAP remains unclear, this study is to investigate the potential essencial role of MCs in acute PAP.

In our pre-experiment, we found that a hypobaric chamber with simulated altitude of 7,000 m to establish an HAPE model in SD rats was better than that 5,000 m. TB positive cells (MCs indicator) in lung tissues showed elevated numbers in all hypoxic groups for varied times (12, 24, 48 and 72 h). Furthermore, results of 12 h were observed better than those of 24, 48 or 72 h. Hence, in order to choose a conditions optimized for animal remodeling induced by hypobaric hypoxia. Our experimental result showed that MCs had increasing number in each HC group(3, 6, 12 and 24 h). Particularly, MCs in HC-12h group had greatest number and were mostly distributed in the pulmonary microvessels. Taken together, these results demonstrated that MCs had the largest number and strongest activity in a hypobaric chamber with simulated altitude of 7000 m at 12 h exposed.

Thereafter, the ultrastructural of MCs was observed in lung tissues derived from rats in HC-12 h groups using TEM. There were alveolar wall swelling, alveolar type II epithelial cell injury, inflammatory cell infiltration, increasing number of MCs, enormous special granules filled in cytoplasm. Based on this, TB staining and TEM assays altogether demonstrated that acute hypoxia could contribute to MCs activation to synthesize reserved and released granules. This result is similar to the existing study (Gulliksson et al. 2010). In addition, TB and TEM results demonstrated that 12h exposure in a hypobaric chamber (simulated altitude of 7000 m) was selected for the experimental conditions of subsequent hypoxic exposure in our research.

The MCs degranulation, one of the reaction mechanism, indicates MCs as the primary effectors that secret His and numerous inflammatory mediators to implicate in immune surveillance and defense. SCG has been reported to inhibit IgE-dependent His and PGD_2 release, further suppressing MCs granulation (Church & Hiroi 1987) (Gulliksson et al. 2010). Its inhibitory effect on MCs degranulation is tissue-specific. SCG prevent MCs from releasing intracellular mediators. Therefore, SCG was selected as experimental drug in our study.

MCs contains various kind of granules such as serine proteinase, Tryptase has been regarded as a vital and specific marker for MCs activation (Atiakshin et al. 2018), and related to the "waterfall effect" of MCs. Chymase is knowingly associated with various reaction mechanisms, such as inflammation and allergy, angiogenesis, oncogenesis and so on (Atiakshin et al. 2019). Furthermore, Chymase has the potential to promote the process of Ang I transforming to Ang II, and activates the renin-angiotensin system. Based on the kinds of proteases in their exocytotic granules, MCs could be classified into two phenotypes, MC_T (contain Tryptase) and MC_{TC} (contain Tryptase and Chymase) (Puxeddu et al. 2005, Zhang et al. 2016). Recent data suggest that MC_T play a vital role in host immune defense against pathogens by elaboration of TNF-α, whereas MC_{TC} participate in angiogenesis and tissue remodeling. The activated MCs release several mediators including Tryptase, Chymase, IL-6, 5-HT, His, resulting in the “waterfall effect” of MCs through different pathways. In this work, WB and IF assays both demonstrated that under the stimulation of acute hypobaric hypoxia environment, the expression of Tryptase and Chymase (M_{CT} and MC_{TC}) in lung tissue is significantly increased, and the expression of both proteins (both types of MCs) was decreased after SCG pretreatment. In addition, IF assays revealed that Tryptase (red) and Chymase (green) positive cells in HC group were extensively expressed in the same cells. These results indicate that acute hypoxia could lead to the increased quantity, enhanced activity, and degranulation of both types MCs (most MC_{TC} type MCs, distributed near microvessels). Taken together our study suggest that MCs may play a "sentry" role in response to hypoxia stress.

IL-6 as a multifunctional inflammatory cytokine, plays a vital role in an acute severe systemic inflammatory response known as “cytokine storm” (Tanaka et al. 2016). As have been reported, MCs can release IL-6 via activation of signal pathways, such as p38, MAPK and Akt, in allergic inflammation(Galli & Tsai 2012). The MCs-derived IL-6 promote the MCs activation and ‘waterfall effect’ of degranulation. Similarly, MCs released Tryptase directly or indirectly activates MCs by PAR-2 to increase their recruitment and degranulation, thereby producing that ‘waterfall effect’ (Liu et al. 2016). Our results indicated that acute hypoxia stimulated MCs release of IL-6. Combined with former results of Tryptase, it suggest that acute hypoxia led to MCs increase and release of Tryptase and IL-6. They promoted MCs rapid recruitment, activation, explosive degranulation as well as the sequential "cascade effect" of releases of biologically active mediators, which amplified the signal of hypoxia stimulation and MCs activation.

Numerous immunological mediators are released after the MCs activation, such as His, 5-HT, Chymase and renin, which could, directly or indirectly, increase the constriction of the pulmonary blood vessels (Xu et al. 2018). 5-HT can enhance the vasoconstriction effect of NE (Noradrenaline) and other substances, which can cause severe spasm of small pulmonary vessels, further case the increases of PAP and increases of blood flow resistance. His is a vasoactive substance that causes pulmonary vasoconstriction, increased PAP, and significantly increased local blood flow and vascular permeability through G-protein-PLC (Phospholipase C) signaling pathway and Ca^{2+} concentration regulation. In our results revealed that lung tissues had elevated levels of 5-HT, His and Ang II under acute hypoxia stree, and decreased levels of 5-HT, His after SCG pretreatment.

We found that acute hypobaric hypoxia contributed to the increased quantity, activity, and degranulation of MCs and SCG treatment showed attenuated PAP elevation under acute hypoxia.

Our findings implied that there is a possible mechanism of acute hypoxia cause rapid recruitment of MCs, activation, and explosive degranulation to release Tryptase, Chymase, IL-6, His, 5-HT, and Ang II, which further contributed to pulmonary microvascular contraction and increase in PAP. This work extends the knowledge about MCs, providing a potential profile of MCs as an alternative treatment for HAPE related increased pulmonary artery pressure.

Despite these promising results, questions remain. Further study should be undertaken to investigate the mechanism of PAP increase development induced by MCs activation and degranulation under acute hypoxia and of PAP increase prevention by SCG.

Funding. This study was supported by the National Natural Science Foundation of China (No. 81560301，81660707); Application and Basic Research of Qinghai Province Science and Technology Department. (No. 2020-ZJ-772); Young and Middle-aged Foundation Project of Medical College of Qinghai University (No. 2017-KYZ-04). Qinghai Province“High-end Innovative Talents and Thousand Talents Program” Leading Talent Project

Acknowledgments. We’d like to show our great appreciations to Dr. Wei Zhang, Shuang Ma (Research Center for High Altitude Medicine Qinghai University), Professor Mingxia Chen (Xi'an Jiaotong University), Dr. Zhenxing Fu (University of California), and Dr.Yaozong Wu (Applied Protein Technology Co., Ltd., Shanghai, P. R. China) for their contributions to the technical and experimental assistances in this study.

Conflicts of interest. The authors declare that there is no conflict of interest between them or their various institutions.

References

Aiello RJ, Bourassa PA, Zhang Q, Dubins J, Goldberg DR et al. (2017): Tryptophan hydroxylase 1 Inhibition Impacts Pulmonary Vascular Remodeling in Two Rat Models of Pulmonary Hypertension. J Pharmacol Exp Ther. 360: 267-279.

Atiakshin D, Buchwalow I, Samoilova V, Tiemann M. (2018): Tryptase as a polyfunctional component of mast cells. Histochem Cell Biol. 149: 461-477.

Atiakshin D, Buchwalow I, Tiemann M. (2019): Mast cell chymase: morphofunctional characteristics. Histochem Cell Biol. 152: 253-269.

Burtscher M, Gatterer H, Faulhaber M, Burtscher J. (2014):Acetazolamide pre-treatment before ascending to high altitudes: when to start. Int J Clin Exp Med. 7: 4378-83.

Chumanevich A, Wedman P, Oskeritzian CA. (2016):Sphingosine-1-Phosphate/Sphingosine-1-Phosphate Receptor 2 Axis Can Promote Mouse and Human Primary Mast Cell Angiogenic Potential through Upregulation of Vascular Endothelial Growth Factor-A and Matrix Metalloproteinase-2. Mediators Inflamm. 2016: 1503206.

Church MK, Hiroi J. (1987): Inhibition of IgE-dependent histamine release from human dispersed lung mast cells by anti-allergic drugs and salbutamol. Br J Pharmacol. 90: 421-9.

Galli SJ, Tsai M. (2012):IgE and mast cells in allergic disease. Nat Med. 18: 693-704.

Gulliksson M, Carvalho RF, Ullerås E, Nilsson G. (2010): Mast cell survival and mediator secretion in response to hypoxia. PLoS One. 5: e12360.

Hendriksen E, van Bergeijk D, Oosting RS, Redegeld FA. (2017):Mast cells in neuroinflammation and brain disorders. Neurosci Biobehav Rev. 79: 119-133.

Kosanovic D, Dahal BK, Peters DM, Seimetz M, Wygrecka M et al. (2014): Histological characterization of mast cell chymase in patients with pulmonary hypertension and chronic obstructive pulmonary disease. Pulm Circ. 4: 128-36.

Levick SP, Widiapradja A. (2018): Mast Cells: Key Contributors to Cardiac Fibrosis. Int J Mol Sci. 19 .

Li Y, Zhang Y, Zhang Y. (2018): Research advances in pathogenesis and prophylactic measures of acute high altitude illness. Respir Med. 145: 145-152.

Liu X, Wang J, Zhang H, Zhan M, Chen H et al. (2016):Induction of Mast Cell Accumulation by Tryptase via a Protease Activated Receptor-2 and ICAM-1 Dependent Mechanism. Mediators Inflamm. 2016: 6431574.

Lotfi-Emran S, Ward BR, Le QT, Pozez AL, Manjili MH et al. (2018): Human mast cells present antigen to autologous CD4(+) T cells. J Allergy Clin Immunol. 141: 311-321.e10.

Luks AM, Auerbach PS, Freer L, Grissom CK, Keyes LE et al. (2019): Wilderness Medical Society Clinical Practice Guidelines for the Prevention and Treatment of Acute Altitude Illness: 2019 Update. Wilderness Environ Med. 30: S3-S18.

Luo Y, Wang Y, Lu H, Gao Y. (2014): 'Ome' on the range: update on high-altitude acclimatization/adaptation and disease. Mol Biosyst. 10: 2748-55.

Ji QR, Zhang Y, Zhang H, Liu J, Cao CZ, Yuan ZY, Ma QQ, Zhang W.(2020):Effects of β-adrenoceptor activation on haemodynamics during hypoxic stress in rats. Experimental Physiology. 2020:1–9.

MacLean MR, Dempsie Y. (2009): Serotonin and pulmonary hypertension--from bench to bedside. Curr Opin Pharmacol. 9: 281-6.

Maggiorini M. (2010):Prevention and treatment of high-altitude pulmonary edema. Prog Cardiovasc Dis. 52: 500-6.

Mandegar M, Fung YC, Huang W, Remillard CV, Rubin LJ, Yuan JX. (2004): Cellular and molecular mechanisms of pulmonary vascular remodeling: role in the development of pulmonary hypertension. Microvasc Res. 68: 75-103.

Möllerherm H, Branitzki-Heinemann K, Brogden G, Elamin AA, Oehlmann W et al. (2017):Hypoxia Modulates the Response of Mast Cells to Staphylococcus aureus Infection. Front Immunol. 8: 541.

Novotný T, Krejčí J, Malíková J, Švehlík V, Wasserbauer R et al. (2015): Mast cell stabilization with sodium cromoglycate modulates pulmonary vessel wall remodeling during four-day hypoxia in rats. Exp Lung Res. 41: 283-92.

Puxeddu I, Ribatti D, Crivellato E, Levi-Schaffer F. (2005): Mast cells and eosinophils: a novel link between inflammation and angiogenesis in allergic diseases. J Allergy Clin Immunol. 116: 531-6.

Rhind GB, MacNee W, Flenley DC. (1986):Disodium cromoglycate fails to prevent the rise in pulmonary artery pressure in hypoxic chronic bronchitis and emphysema. Eur J Respir Dis. 68: 58-63.

Ribatti D. (2018): The Staining of Mast Cells: A Historical Overview. Int Arch Allergy Immunol. 176: 55-60.

Ribatti D, Tamma R, Vacca A. (2019):Mast Cells and Angiogenesis in Human Plasma Cell Malignancies. Int J Mol Sci. 20 .

Tanaka T, Narazaki M, Kishimoto T. (2016): Immunotherapeutic implications of IL-6 blockade for cytokine storm. Immunotherapy. 8: 959-70.

Vajner L, Vytásek R, Lachmanová V, Uhlík J, Konrádová V et al. (2006): Acute and chronic hypoxia as well as 7-day recovery from chronic hypoxia affects the distribution of pulmonary mast cells and their MMP-13 expression in rats. Int J Exp Pathol. 87: 383-91.

Xu H, Bin NR, Sugita S. (2018): Diverse exocytic pathways for mast cell mediators. Biochem Soc Trans. 46: 235-247.

Xu J, Wang J, Shao C, Zeng X, Sun L et al. (2018): New dynamic viewing of mast cells in pulmonary arterial hypertension (PAH): contributors or outsiders to cardiovascular remodeling. J Thorac Dis. 10: 3016-3026.

Zhang T, Finn DF, Barlow JW, Walsh JJ. (2016):Mast cell stabilisers. Eur J Pharmacol. 778: 158-68.

Zhang W, Shibamoto T, Cui S, Takano H, Kurata Y. (2009): 7-nitroindazole, but not L-NAME or aminoguanidine, attenuates anaphylactic hypotension in conscious rats. Shock. 31: 201-6.

Figure legends

Figure 1. Conditions of rats modeling for hypobaric hypoxia were optimized by TB staining. (A) TB staining images of NC and HC groups at varied breeding times (3, 6, 12, and 24 h). Scale bar indicates 50 μm and images are shown at a magnification of 40×; (B) TB positives cells (MCs) were counted at varied altitude at different hypoxia exposure times. * $P < 0.05$ versus N group; $^{\#}$ $P < 0.05$ versus 3 h group; $^{\blacktriangle}P < 0.05$ versus 6 h; $^{\bullet}P < 0.05$ versus 12 h, $P < 0.05$.

Figure 2. TEM images of the morphology of lung tissues. (A) The morphology of NC-12h group normal alveolar type II epithelial cells. (B) (C) (D) The morphology of pathological alveolar type II epithelial cells and (E)-(H) MCs in HC-12h group. Blue arrows indicate normal lamellar body. Yellow arrows indicate damage and evacuation of lamellar bodies. Green arrows indicate the mitochondria swollen in oval or round shape. Pink arrow indicates erythrocyte, neutrophils, eosinophils et al. aggregated in capillaries. Red arrows indicate that the outer membrane structure of some granules disappeared. Scale bar indicates 500 nm.

Figure 3. The contributing role of acute hypobaric hypoxia to MCs were evaluated by WB assays. (A) Expressions of Tryptase and Chymase in different treated rat groups as analyzed by WB assay. The relative expression of Tryptase (B) and Chymase (C) was counted in different treated rat groups. N12C (2,260 m + NS , 12 h); H3C, H6C, H12C (7,000 m + NS , 3h, 6h, 12h); N12S (2,260 m + SCG , 12 h); H3S, H6S, H12S (7,000 m + SCG ,3 h, 6h, 12h). * $P < 0.05$ versus HC group; $^{\#}$ $P < 0.05$ versus 3h group; $^{\blacktriangle}P < 0.05$ versus 6h group. The relative expression of Tryptase (D) and Chymase (E) was counted in different treated rat groups. * $P < 0.05$ versus N12C group; $^{\#}$ $P < 0.05$ versus H12C group; $^{\blacktriangle}P < 0.05$ versus N12S group.

Figure 4. (A) The contributing role of acute hypobaric hypoxia to MCs were evaluated by IF assay. Observed images of tryptase (red) and chymase (green) in lung tissues of different groups in SD rats

by IF assay. Percent of tryptase (B) and chymase (C) positive cells was counted in different treated rat groups. NC group (2,260 m + NS for 12 h); NSCG group (2,260 m + SCG for 12 h); HC group (7,000 m + NS for 12 h); HSCG group (7,000 m + SCG for 12 h). * $P < 0.05$ versus NC group; $^{\#}$ $P < 0.05$ versus HC group; ▲$P < 0.05$ versus NSCG group.

Figure 5. Contents of IL-6(A), His (B), 5-HT (C), and Ang II (D) in lung tissues from SD rat groups were detected by ELISA assay. SD, Sprague Dawley; ELISA, enzyme-linked immunosorbent assay; NC group (2,260 m + NS for 12 h); NSCG group (2,260 m + SCG for 12 h); HC group (7,000 m + NS for 12 h); HSCG group (7,000 m + SCG for 12 h); SCG, sodium cromoglate. * $P < 0.05$ versus NC group; $^{\#}$ $P < 0.05$ versus HC group; ▲$P < 0.05$ versus NSCG group.

Figure 6. PAP in fully anesthetized SD rats pretreated by SCG were detected at different oxygen concentrations and times. (A) The change of PAP in different groups in rats. (B) PAP difference analysis between groups. $^{\#}$ $P < 0.05$ vesus 0 min; * $P < 0.05$ versus 20.9%O_2 +NS group; ▲$P < 0.05$: 15%O_2+SCG group versus 15%O_2 +NS group, $P < 0.05$.

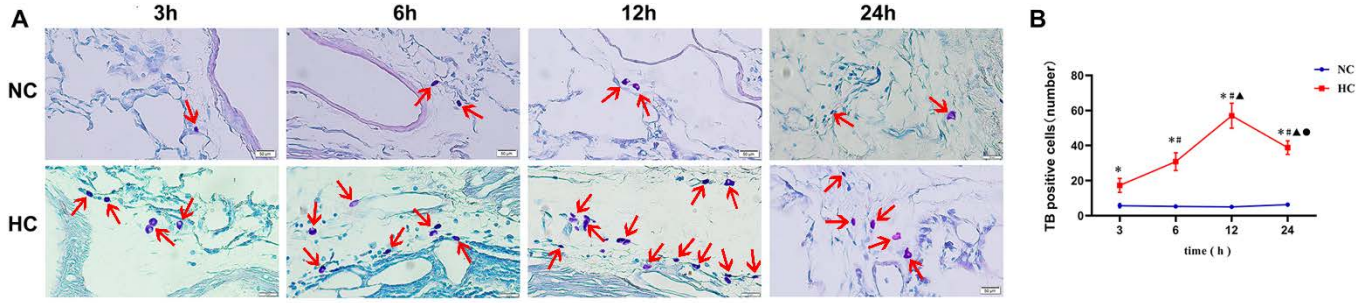

FIGURE 1

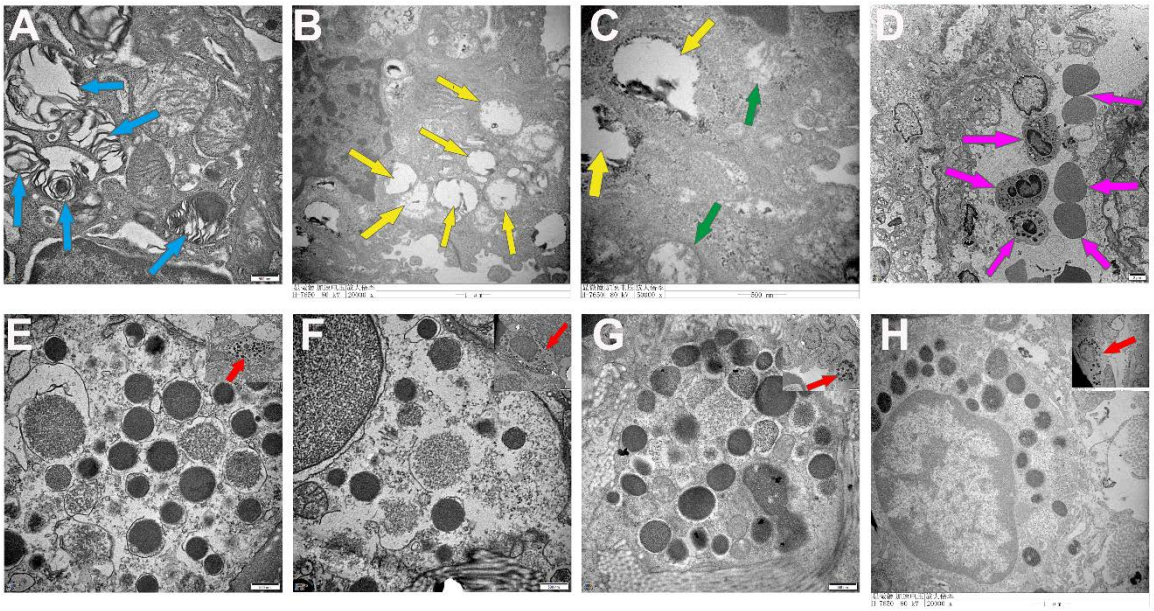

FIGURE 2

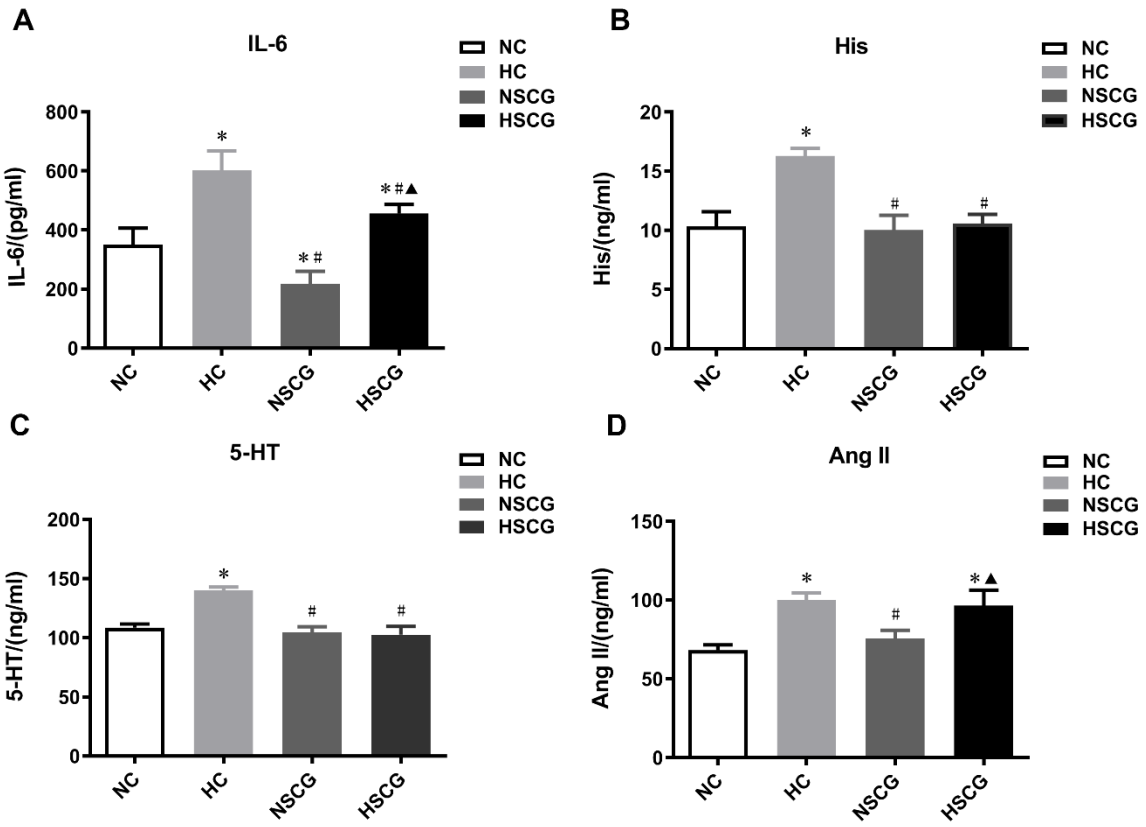

FIG. 5

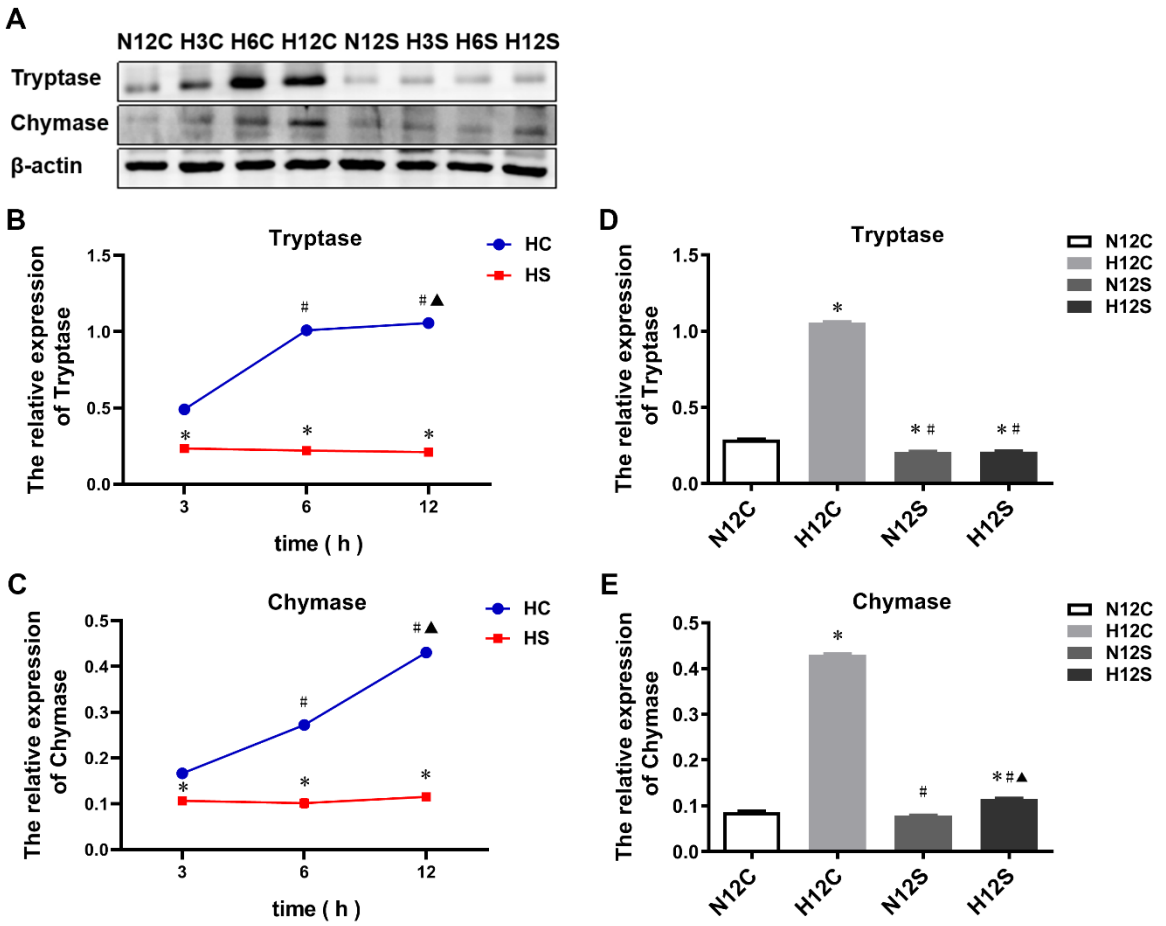

FIFURE 3

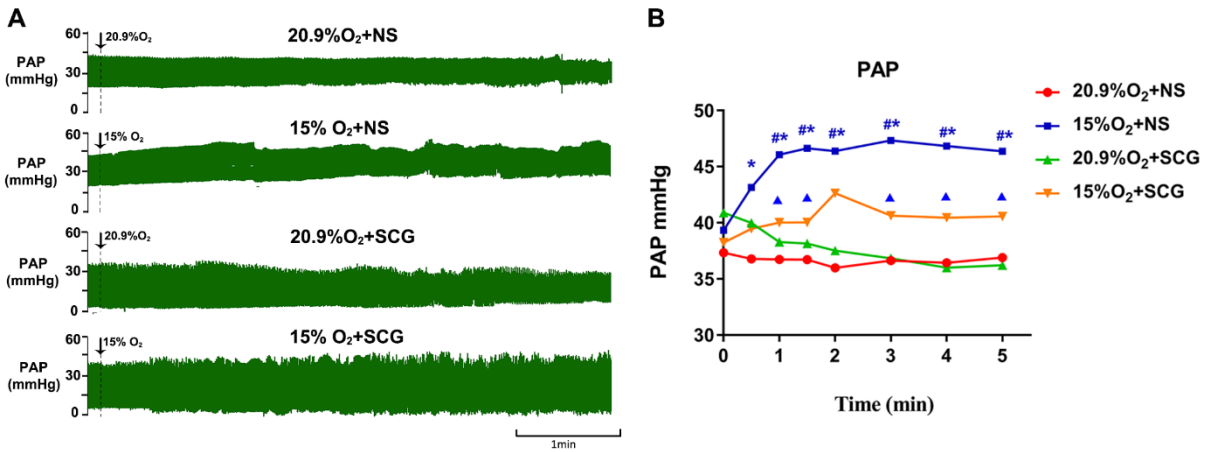

FIGURE 6

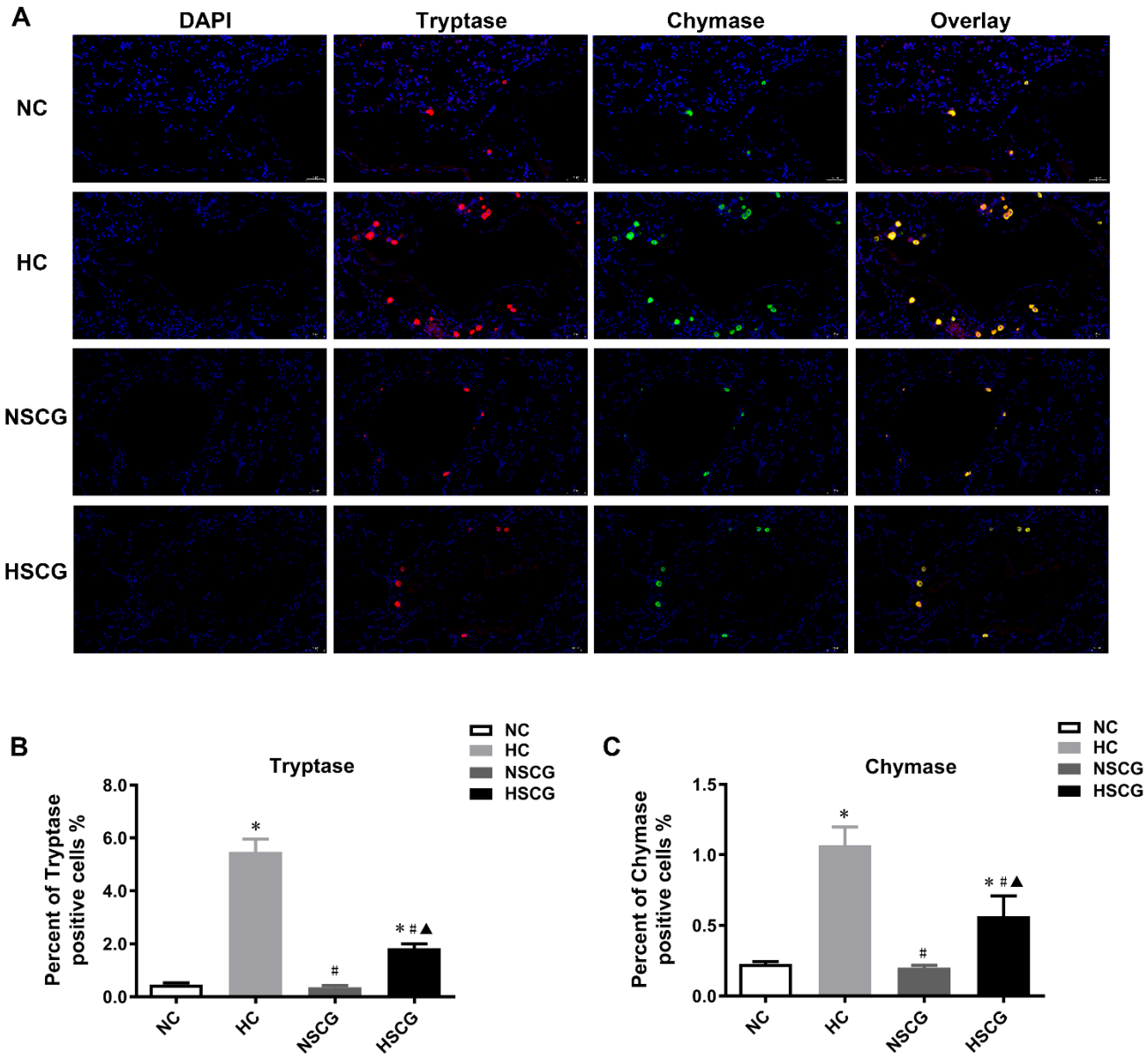
A
DAPI
Tryptase
Chymase
Overlay
NC
HC
NSCG
HSCG
B
Tryptase
Percent of Tryptase positive cells %
8.0
6.0
4.0
2.0
0.0
NC
HC
NSCG
HSCG
C
Chymase
Percent of Chymase positive cells %
1.5
1.0
0.5
0.0

FIGURE 4